Talanta 83 (2011) 1476–1481

Contents lists available at ScienceDirect

Talanta

journal homepage: www.elsevier.com/locate/talanta

Electrochemical properties of a fully integrated, singlewalled carbon nanotube coplanar three-electrode system on glass substrate

Joon-Hyung Jin[a], Joon Hyub Kim[a], Chan Won Park[b], Nam Ki Min[a,c,*]

[a] Department of Biomicrosystem Technology, Korea University, Seoul 136-701, Republic of Korea
[b] Department of Electrical and Electronic Engineering, Kangwon National University, Gangwon-do 200-701, Republic of Korea
[c] Department of Control and Instrumentation Engineering, Korea University, Sejong Campus, Chungnam 339-700, Republic of Korea

ARTICLE INFO

Article history:
Received 16 September 2010
Received in revised form
12 November 2010
Accepted 15 November 2010
Available online 23 November 2010

Keywords:
Electrochemistry
O_2 plasma
Photolithography
Thin-film reference electrode
Transferred CNT

ABSTRACT

Fully integrated carbon nanotube-based three-electrode electrochemical systems were photolithographically prepared on glass substrates and electrochemically characterized. O_2 plasma treatment of the transferred single-walled carbon nanotube (SWCNT) film was voltammetrically optimized in terms of applied plasma power and the elapsed time. The patterned thin film Ag layer was chemically oxidized in an acidic solution for various dip times to form a chlorinated Ag layer. The Nernstian behavior of as-prepared and seven-day-aged Ag/AgCl thin-film electrodes was investigated for optimization, and the electrode's electrochemical attributes were compared to a commercial reference electrode. A quality control evaluation and a performance assessment of the fully integrated SWCNT-transferred sensing systems were performed using cyclic voltammetry. The proposed SWCNT-based three-electrode device exhibited clear electrochemistry under voltammetric conditions, and is therefore a candidate for use in all electrochemical biosensors.

1. Introduction

An electrochemical biosensor is an analytical device in which electrodes serve as transducers that convert a signal resulting from a specific biorecognition event between a ligand and its receptor into a detectable and measurable electrical signal. They have emerged as the most commonly used biosensors in monitoring and diagnosis tests in clinical analysis, and overcome most disadvantages and problems that limit the use of other types of biosensors [1,2]. Electrochemical biosensors offer several advantages over most other biosensors including high sensitivity, specificity for the target analyte, fast response, ability to operate in turbid or colored solutions, ease of use, and the potential to couple with low cost, portable instrumentation [2–4]. Furthermore, the continuous response of an electrode system allows for online control, and applications for a wide range of samples [3,5]. The field of electrochemical biosensors continues to grow at a rapid pace based on these advantages.

The choice of working electrode materials is one of the key issues in the successful fabrication of electrochemical biosensors. The transduction efficiency of electrode transducers determines many of the analytical characteristics of electrochemical biosensors such as sensitivity, selectivity, detection limit, signal stability, and reproducibility. Many materials have been used as electrodes in electrochemical biosensors [6,7]. Metals and carbon are commonly used to prepare electrochemical transducers and supporting substrates. Inert metals such as platinum, gold, and silver have long been used for electrode systems due to their excellent electrical and mechanical properties [6]. Carbon-based materials such as carbon paste, graphite, carbon black, and carbon fiber are also used to construct electrodes. Carbon pastes made of carbon powder and an organic binder are currently the most popular materials for preparation of various electrochemical transducers because of their chemical inertness, relatively wide potential window, low background current, simple construction procedures, and very low cost [6,8–10].

In recent years, carbon nanotube (CNT)-based materials have been introduced for use as electrochemical electrodes. Such materials are the focus of intensive research by analytical chemists for their potential use as novel biosensors based on their unique electrical, mechanical, and structural properties. These properties are ideal for developing different types of nanoscale electrodes and biosensors. Several properties of CNTs make them very promising in terms of developing ultrasensitive and miniaturized electrochemical biosensors for disease diagnosis. Carbon nanotubes can provide strong electrocatalytic activity, low detection limits, increased sensitivity, and decreased overpotentials, coupled with little or no surface fouling [11–13]. In particular, recent studies

* Corresponding author at: Department of Control and Instrumentation Engineering, Korea University, Sejong Campus, Chungnam 339-700, Republic of Korea. Tel.: +82 02 3290 3991; fax: +82 02 925 2296.
E-mail address: nkmin@korea.ac.kr (N.K. Min).

0039-9140/$ – see front matter © 2010 Elsevier B.V. All rights reserved.
doi:10.1016/j.talanta.2010.11.038

demonstrated that CNTs have an outstanding ability to mediate fast electron-transfer kinetics for a wide range of electroactive species when used as electrode materials in chemical reactions [12,13]. Charge transfer reactions at CNTs were found to occur at a faster rate than those at traditional carbon electrodes [14,15]. In addition to enhanced electrochemical reactivity, the chemical functionalization of CNTs can be used to attach almost any desired chemical species to them, which results in enhanced solubility and biocompatibility of the tubes [16,17]. In addition, CNTs can effectively minimize surface fouling of electrochemical devices.

For biosensor applications, carbon nanotube film needs to be deposited onto selective regions of a substrate or be patterned as an electrode. An effective method for fabricating patterned CNT electrodes is the direct growth of CNTs onto substrate with prepatterned catalytic metal films [18,19]. An array of MWCNTs grown from photolithography and e-beam-patterned Ni spots have been used to detect DNA hybridization [20]. More recently, immunosensors using patterned CNTs have been developed to detect pathogens [21,22].

In [18–22], substrates were selectively patterned with catalyst metals, and carbon nanotubes were grown in the pre-patterned areas using the chemical vapor deposition (CVD) technique. However, these techniques produce films with poor adhesion and low material purity. Moreover, since CVD growth requires high temperatures (600–1200 °C), the substrates are restricted to high melting point semiconductors or insulators. This limitation eliminates the use of low cost substrates such as soda-lime glass and plastics. Therefore, there is a need to develop more convenient methods for patterning carbon nanotube films with adequate adhesion to allow the use of low melting point materials as substrates. There are relatively few studies reported in the literature describing techniques for fabricating electrochemical biosensors based on CNT electrodes patterned at low temperatures.

In this study, we demonstrate a co-planar single wall carbon nanotube (SWCNT)-based three-electrode system that is fully microfabricated on the glass substrate. The silver/silver chloride thin film reference electrode and the SWCNT-modified platinum thin film (before and after the SWCNT transfer) were electrochemically characterized in view of biosensor fabrication and potential applications.

2. Materials and methods

2.1. Materials

We used hexa methylene disilazane (HMDS) as an adhesion promoter; AZ1512 as a positive photoresist (PR) material; positive PR developer (CD30); negative PR (DNR-L300); and dichlorobenzene (DCB) (99.0%) as a solvent for the SWCNTs. These chemicals were purchased from Daejung Chemicals and Metals Co. Ltd. (Republic of Korea). Negative PR developer (AZ 500 MIF, Daejung Chemicals and Metals Co. Ltd., Republic of Korea) was diluted with deionized (DI) water in a volume ratio of 2:1. Buffered oxide etchant (BOE) for etching silicon dioxide was prepared by dilution of the BOE with DI water in a volume ratio of 6:1. Nitric acid (60.0%) was diluted with DI water in a volume ratio of 1:9 for the desorption of SWCNTs from the filter paper. A 1 M solution of hydrochloric acid (35.0%) was prepared for chemical oxidation of the evaporated silver thin film. SWCNTs (ASP-100F) were purchased from Hanwha Nanotech Chemical Co. Ltd. (Republic of Korea). Chemicals and materials were used without further purification unless otherwise stated.

2.2. Apparatus

Silicon dioxide and nitride films were deposited using plasma-enhanced chemical vapor deposition (PECVD) (Plasmalab 800 Plus, Oxford, England). Nitride etching was performed using reactive ion etching (RIE) (Advanced Vacuum & STS, Advanced RIE, USA). Electrochemical measurements were performed using an electrochemical workstation composed of a potentiostat/galvanostat (M263A, Princeton Applied Research, USA), an IBM compatible PC, and a lab-made electrochemical cell. Pt wire (99.95%) and potassium saturated Ag/AgCl electrode material (Sigma–Aldrich, USA) were used as the counter and the reference electrodes, respectively. A Direct-Q pure water system (Millipore, USA) was used to prepare DI water with a resistivity of 18.2 MΩ cm for aqueous media.

2.3. Fabrication procedures

2.3.1. Preparation of a homogeneous SWCNT film for transfer

First, 3 mg of SWCNTs were dispersed in 150 mL of DCB with sonication for 20 min. The resulting homogeneous SWCNT solution was chilled for 1 h. After being centrifuged, 5 mL of the supernatant solution was filtered through Whatmann no. 6809-5002 filter paper (20 nm of particle retention), and then the used filter paper was immersed in a dilute nitric acid solution to separate the SWCNT adsorbate from the filter paper. The isolated SWCNTs were shifted to the fully integrated three-electrode substrate and dried for 1 h at 80 °C.

2.3.2. Fabrication of a fully integrated electrochemical three-electrode system based on a glass substrate and activation of the transferred SWCNTs

A pyrex glass wafer with a diameter of 4 in was thoroughly cleaned in boiled ethanol to remove organic traces and rinsed with DI water. Three Pt electrodes were patterned on the glass substrate using the lift-off process. Promoter HMDS was spin-coated on the substrate at 4000 rpm followed by a positive PR coating, and the substrate was then developed in a dilute MIF solution for 30 s. Pt film was evenly deposited on the PR-patterned glass substrate to a thickness of 200 nm using direct current (DC) magnetron sputtering at 150 W. The flow rate of Ar was 30 sccm at 5 mPa. The Pt film coated on the PR was easily removed by dipping it in acetone for 5 min.

A silver layer for a thin-film reference electrode was directly formed on the smallest of the three Pt thin films. First, a negative PR (DNR-L300, Daejung Chemicals and Metals Co. Ltd., Republic of Korea) was spin-coated on the Pt-patterned glass substrate at 3000 rpm for 60 s. After curing under UV illumination for 21 s, the substrate was developed in a negative PR developer and baked on a hot plate for 90 s. Secondly, silver film was uniformly evaporated onto the negative PR-patterned substrate to a thickness of 200 nm using an electron beam evaporator. Finally, the substrate was immersed in acetone to remove the PR.

Two passivation layers were used to selectively modify the sensing electrode with the transferred SWCNT. The silicon dioxide layer was deposited to a thickness of 200 nm on the three-electrode substrate at 0.9 Torr and 20 W (deposition speed < 45 nm min^{-1}), followed by deposition of a 300 nm-thick nitride layer at 0.9 Torr and 50 W (deposition speed < 11 nm min^{-1}). The nitride layer was etched at 0.05 Torr and 50 W for 6 min (etching speed < 50 nm min^{-1}) after development of a photolithographically patterned negative PR to prepare the windows for the three metal thin-film electrodes. The silicon dioxide layer deposited on the working electrode was removed by immersion of positive PR-patterned substrate in BOE for 7 s. Ultimately, as shown in Fig. 1, there were three windows available. Two of them (with silicon dioxide-layered nitride windows) were used as reference and counter electrodes, respectively. The other electrode, positioned in the center, had a fully opened window and was used as a working electrode.

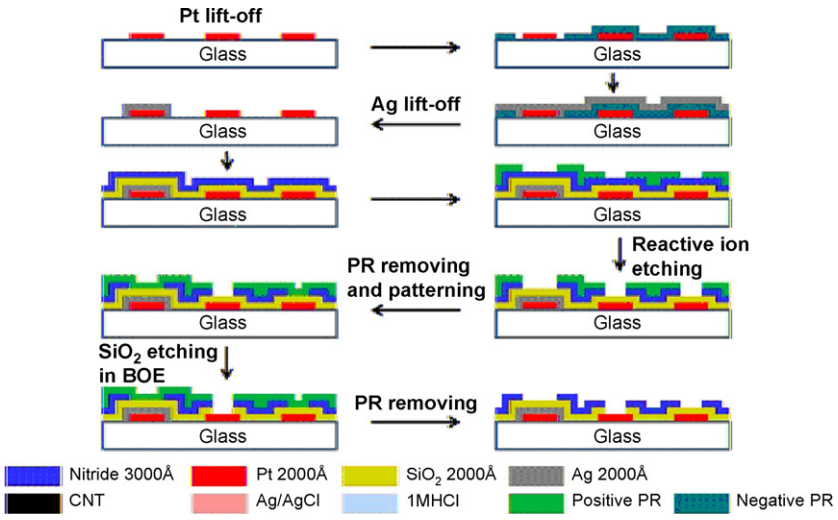

Fig. 1. Fabrication procedure of an electrochemical three-electrode system based on CNT patterning.

The previously prepared SWCNT layer was transferred onto the substrate. Positive PR was spin-coated on the substrate at 2000 rpm, followed by PR patterning under UV illumination for 23 s and baking on a hot plate for 60 s. Then, the resulting layer was developed in a positive PR developer for 30 s. The patterned PR acted as a masking material in a subsequent step of O_2 plasma etching at 60 W for 3 min (the flow rate of O_2 was 10 sccm) to remove the unwanted SWCNT layer formed on the reference and counter electrodes. Afterward, the PR was removed in acetone. The remaining transferred SWCNTs on the working electrode were activated by an O_2 plasma treatment at 20 W for 25 s (the flow rate of O_2 was 30 sccm).

Silicon dioxide layers on the reference and the counter electrodes were etched off by immersing the substrate in BOE for 7 s. The final step was to chlorinate the Ag layer in 1 M HCl solution. Thirty minutes of dip time was enough to provide a thin-film Ag/AgCl reference electrode with acceptable Nernstian behavior. Fig. 2 shows the complete procedure of O_2 plasma-based activation of the transferred SWCNTs and the subsequent chlorination of Ag to prepare a thin-film Ag/AgCl reference electrode.

3. Results and discussion

Scanning electron microscopy (SEM) images of a fully integrated electrochemical three-electrode system are shown in Fig. 3(a). Arabic numbers one, two, and three denote the reference, counter, and working electrodes, respectively. A small area of the reference electrode enabled an intrinsically reduced potential drop (IR drop). Extreme cases of huge IR drops can lead to functional failures of the micro-electrode system. A counter electrode having a relatively large surface area allowed a wide range of current between the counter and working electrodes, which means that the operational potential had a wide input range. Additionally, the SWCNT network on the working electrode provided the electrode with a better environment for the immobilization of various biomacromolecules.

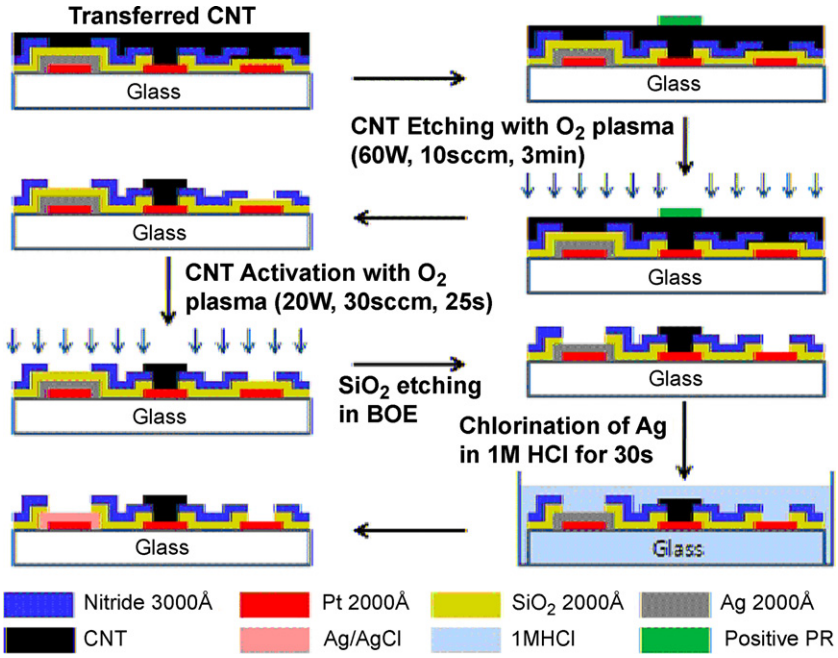

Fig. 2. CNT patterning for modification of Pt thin film working electrode, and the chlorination of silver thin film for the formation of Ag/AgCl following the activation of the CNT-patterned electrode.

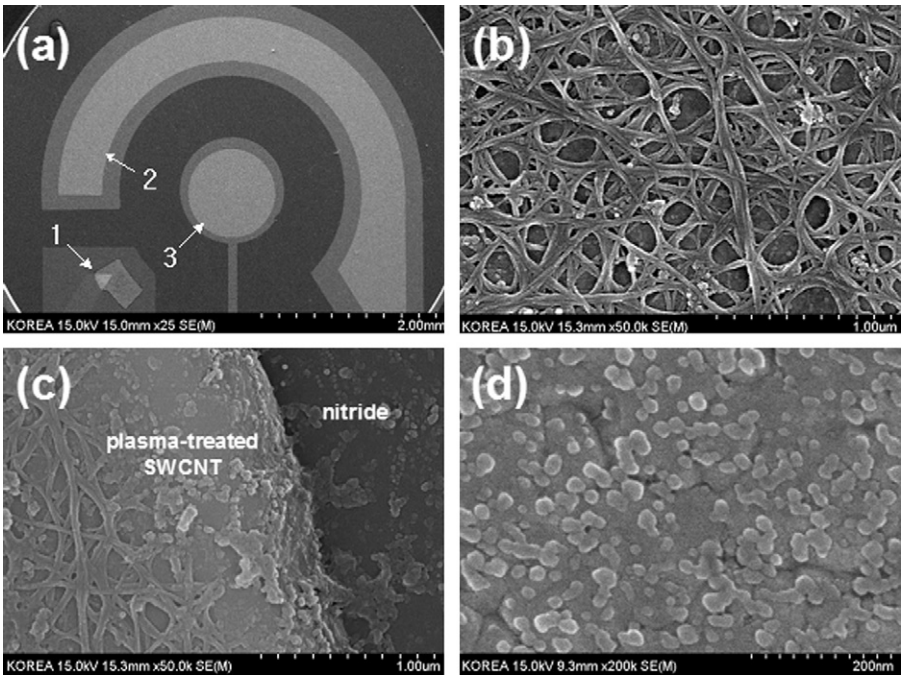

Fig. 3. SEM images of (a) a fully integrated CNT-patterned three-electrode system. 1, 2, and 3 denote the reference, counter, and working electrodes, respectively; (b) a magnified CNT-patterned working electrode in which the CNT network is clearly shown.

Fig. 3(b) and (c) is the SWCNT-transferred sensing electrodes before and after plasma treatment, respectively. Granular surface of the Ag/AgCl thin-film reference electrode is also shown in Fig. 3(d).

The transferred SWCNT film required plasma treatment. Cyclic voltammogram a in Fig. 4 shows that peak potential separation ΔE of the cyclic voltammogram of a bare SWCNT-modified electrode taken from a 3 M KCl solution containing 10 mM potassium ferricyanide was larger than 500 mV with poor peak currents. However, the other cyclic voltammograms (b–f) show that plasma-treated SWCNT electrodes were basically diffusion-controlled [23]. The value of ΔE decreased until the applied plasma power reached 30 W. If the applied plasma power were more than 30 W, the ΔE would increase again. Total anodic and total cathodic peak currents kept increasing as long as the power increased, from 10 W to 50 W. Table 1 summarizes two major factors: the applied O_2 plasma power, and the elapsed time affecting ΔE and the corresponding peak currents. The value of ΔE was significantly reduced by the plasma treatment to the transferred SWCNT; however, it would increase if more than 30 W of plasma power were applied. Maximum Faradaic peak currents were observed at around 20 W of plasma power. This means that at a lower power than 20 W, the SWCNT was not fully activated. This might be because the organic solvent previously used to prepare the homogeneous SWCNT solution could not be sufficiently removed at low power. However, too much high power can cause destruction of the unique structure of the SWCNTs, causing them to be less conductive. Similarly, Faradaic peak currents decreased as the elapsed time of the plasma treatment increased.

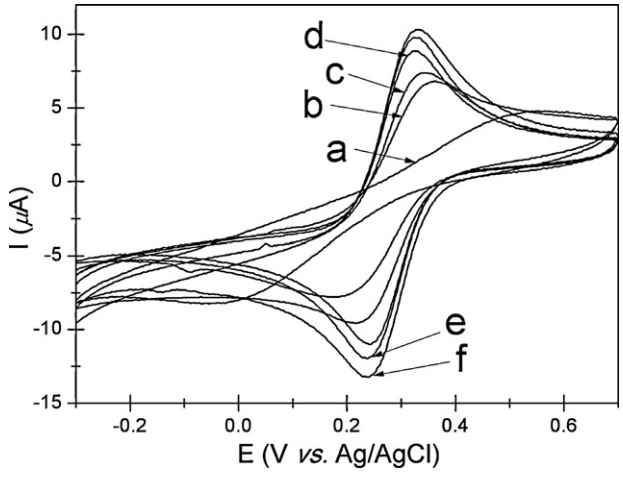

Fig. 4. Cyclic voltammograms of O_2 plasma-treated CNT working electrodes in a 3 M of KCl solution containing 10 mM $K_3Fe(CN)_6$ at a scan rate of 100 mV s^{-1}. The CNT-transferred working electrodes were exposed to O_2 plasma at (a) 0 W, (b) 10 W, (c) 20 W, (d) 30 W, (e) 40 W, and (f) 50 W. The exposition time was 20 s.

The current response of the bare Pt thin-film electrode of the integrated system was recorded as a function of applied potential when the Ag/AgCl thin-film was used as a reference electrode. There was no difference in ΔE or the peak current between an as-prepared Ag/AgCl and a seven-day-aged Ag/AgCl thin-film. The redox reaction of potassium ferricyanide on the bare Pt electrode is diffusion-controlled, both with a commercial reference electrode

Table 1
Dependence of electrochemical variables on electrical power and elapsed time applied to O_2 treatment of CNT working electrodes.

	$\lvert E_{pc} - E_{pa} \rvert$ (mV)	I_{pc} (μA)	I_{pa} (μA)
O_2 plasma power (W)[a]			
0	568	2.04	5.20
10	82.5	11.4	11.0
20	116	15.8	18.4
30	90.4	12.9	12.7
40	124	9.34	9.01
50	189	8.74	7.55
Elapsed time (s)[b]			
0	568	2.04	5.20
10	112	17.2	17.1
20	116	15.8	18.4
40	96.3	12.3	11.9
60	96.3	10.9	10.6

[a] Elapsed time is 20 s.
[b] Plasma power is 20 W.

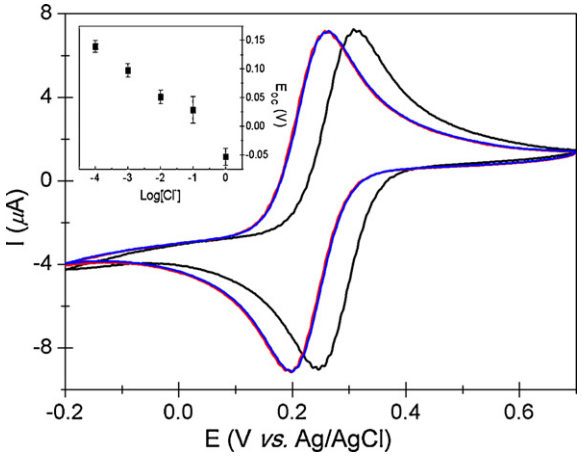

Fig. 5. Cyclic voltammograms of Pt electrode in a 3 M KCl solution containing 10 mM $K_3Fe(CN)_6$ when a commercially available reference electrode (black line), an as-prepared Ag/AgCl thin film (red line), and a one week-incubated Ag/AgCl thin film (blue line) reference electrode were used. The Nernstian slope of the as-prepared Ag/AgCl thin film reference electrode approximates 48.2 mV per chloride ion concentration decade. (For interpretation of the references to color in this figure legend, the reader is referred to the web version of the article.)

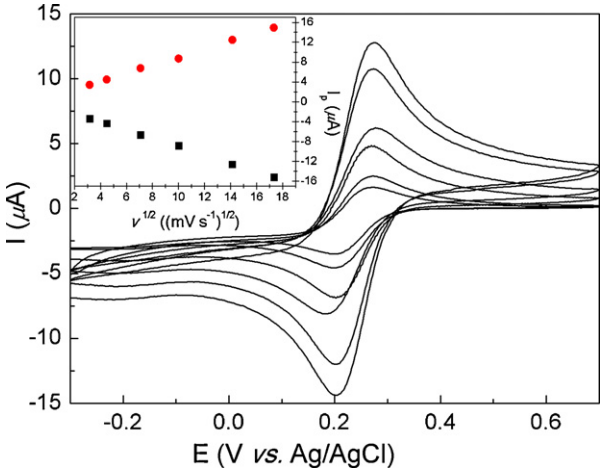

Fig. 7. Cyclic voltammograms of an activated CNT electrode in 3 M KCl solution containing 10 mM $K_3Fe(CN)_6$ as a working electrode in a fully integrated CNT-based three-electrode system. The scan rates are 10 mV s^{-1}, 20 mV s^{-1}, 50 mV s^{-1}, 100 mV s^{-1}, 200 mV s^{-1}, and 300 mV s^{-1}. The plots of anodic and cathodic peak currents as functions of the square root of the scan rates show a linear relationship (inset).

and with fabricated Ag/AgCl thin-film. Fig. 5 also shows that when thin-film Ag/AgCl was used, a downshift of voltammograms in peak potentials by 50 mV. The half-cell reaction on Ag/AgCl thin-film is $AgCl(s) + e^- \rightarrow Ag(s) + Cl^-$, and the corresponding Nernst equation is $E = E^0 + 0.059 \log(1/[Cl^-])$ where E^0 represents the standard potential or, more accurately, the formal potential (i.e., only the chloride ion concentration determines the open circuit potential E_{OC}). The inset of Fig. 5 shows a plot of E_{OC} versus the logarithmic chloride ion concentration. The mean Nernstian slope is 48.2 mV $decade^{-1}$ with good stability.

The dip time in a dilute hydrochloric acid solution for chlorination of the Ag layer is a crucial factor affecting the electrochemical cell potential. Eight Ag/AgCl thin films were prepared by varying the immersion time for chlorination from 10 s to 180 s. The formal potential (defined as the arithmetic mean of anodic and cathodic peak potentials) for a ferrocyanide/ferricyanide redox couple moves to regions of more positive potential that is finally 230 mV, with a 10% increase in peak current, until the dip time reaches 90 s. However, if the dip time is much greater than 90 s (e.g., 180 s as shown in cyclic voltammogram a in Fig. 6), the formal potential moves back to regions of less positive potential, and was observed in our experiment at much less than 230 mV.

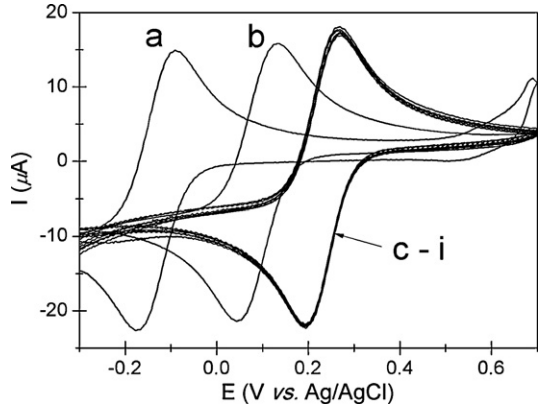

Fig. 6. Cyclic voltammograms of a bare Pt electrode in a 3 M KCl solution containing 10 mM $K_3Fe(CN)_6$ with various prepared reference electrodes. The time durations of chlorination in a 1 M HCl solution for preparing reference electrodes were (a) 180 s, (b) 0 s, (c) 10 s, (d) 20 s, (e) 30 s, (f) 40 s, (g) 50 s, (h) 60 s, and (i) 90 s.

The electrochemical quality control of a fully integrated SWCNT-transferred three-electrode system prepared at an optimized condition is shown in Fig. 7. Cyclic voltammograms of the SWCNT-based sensing electrode in 3 M KCl solution containing 10 mM potassium ferricyanide exhibit a perfect diffusion-controlled reversible reaction, showing 70 mV of ΔE at all scan rates. The Randles plot shown in inset of Fig. 7 also indicates that the curves of peak currents versus the square root scan rates are linear. The active areas of the electrode, taken from the anodic and cathodic slopes, were approximately 0.35 mm^2 and 0.36 mm^2, respectively. This implies that because the geometric area of the working electrode was 0.79 mm^2, 44–45% of the electrode area was still electrochemically active with the SWCNT-transferred sensing electrode.

4. Conclusions

A fully integrated SWCNT-patterned three-electrode system was successfully fabricated on a glass substrate. The transferred SWCNT film must be activated using O_2 plasma treatment to eliminate organic contaminants from the fabrication procedure for the SWCNT transfer. 20 W of plasma power and 20 s of elapsed time is recommended as the optimized plasma condition under which the narrowest ΔE and the largest peak currents were observed. The best condition for a stable and reproducible thin-film Ag/AgCl electrode when 1 M hydrochloric acid solution was used to chemically oxidize an Ag layer was to dip the Ag layer into the solution for 10 s to form a silver chloride layer. Reproducible Nernstian slopes verified excellent reproducibility of the fabricated Ag/AgCl thin-film. An identical cyclic voltammogram of the electrode system (even 7 days later) under aerobic conditions confirmed a relatively high resistance against natural aging of the system. Plasma treatment can activate or simultaneously deactivate the transferred SWCNT film. If more precise control of the size of the CNT were available, a much larger active area of the sensing electrode would be possible.

More importantly, carbon nanotubes (the most promising immobilization matrix) have larger electrical and heat conductivities than normal metals by orders of magnitude. The nanostructured CNT-modified electrode surface is basically very rough; thus, it can be easily functionalized with biosensor materials. In addition, it has a large surface-to-volume ratio that results in a better environment for immobilizing biomacromolecules, including various enzymes, antibodies, and nucleic acids, and in greatly

enhanced sensitivity. A fully integrated SWCNT-patterned three-electrode system based on a glass substrate can make it possible to create a cost-effective, highly sensitive CNT incorporated biocompatible device. Thus, the proposed nanostructured CNT-modified electrode system can be applied in a variety of biosensor industries.

Acknowledgments

This work was supported by Grant No. K20601000002-07E0100-00210 from Korea Foundation for International Cooperation of Science & Technology.

References

[1] D. Grieshaber, R. MacKenzie, J. Voros, E. Reimhult, Sensors 8 (2008) 1400–1458.
[2] M. Mehrvar, M. Abdi, Anal. Sci. 20 (2004) 1113.
[3] M.S. Wilson, Anal. Chem. 77 (2005) 1496–1502.
[4] O.A. Sadik, A.O. Aluoch, A. Zhou, Biosens. Bioelectron. 24 (2009) 2749–2765.
[5] D. Ivnitski, I. Abdel-Hamid, P. Atanasov, E. Wilkins, S. Stricker, Electroanalysis 12 (2000) 317–325.
[6] S. Zhang, G. Wright, Y. Yang, Biosens. Bioelectron. 15 (2000) 273–282.
[7] S. Sotiropoulou, V. Gavalas, V. Vamvakaki, N.A. Chaniotakis, Biosens. Bioelectron. 18 (2003) 211–215.
[8] I. Svancara, K. Vytras, J. Barek, J. Zima, Anal. Chem. 31 (2001) 311–345.
[9] I. Svancara, K. Vytras, K. Kalcher, A. Walcarius, J. Wang, Electroanalysis 21 (2009) 7–28.
[10] Z. Jiri, S. Ivan, B. Jiri, V. Karel, Anal. Chem. 39 (2009) 204–227 (24).
[11] J. Wang, Electroanalysis 17 (2005) 7–14.
[12] K. Balasubramanian, M. Burghard, Anal. Bioanal. Chem. 385 (2006) 452–468.
[13] Q. Zhao, Z. Gan, Q. Zhuang, Electroanalysis 14 (2002) 1609–1613.
[14] P.J. Britto, K.S.V. Santhanam, P.M. Ajayan, Bioelectrochem. Bioenerg. 41 (1996) 121–125.
[15] J.M. Nugent, K.S.V. Santhanam, A. Rubio, P.M. Ajayan, Nano Lett. 1 (2001) 87–91.
[16] E. Katz, I. Willner, ChemPhysChem 5 (2004) 1084–1104.
[17] K. Balasubramanian, M. Burghard, Small 1 (2005) 180–192.
[18] T. Gabay, M. Ben-David, I. Kalifa, R. Sorkin, Z.R. Abrams, E. Ben-Jacob, Y. Hanein, Nanotechnology 18 (2007) 6.
[19] Y.H. Yun, V. Shanov, M.J. Schulz, Z. Dongc, A. Jazieh, W.R. Heinemand, H.B. Halsall, D.K.Y. Wong, A. Bange, Y. Tuf, S. Subramaniam, Sens. Actuators B 120 (2006) 298–304.
[20] J. Li, H.T. Ng, A. Cassell, W. Fan, H. Chen, Q. Ye, J. Koehne, J. Han, M. Meyyappan, Nano Lett. 3 (2003) 597–602.
[21] Y.H. Yun, A. Bange, W.R. Heineman, H.B. Halsall, V.N. Shanov, Z. Dong, S. Pixley, M. Behbehani, A. Jazieh, Y. Tue, D.K.Y. Wong, A. Bhattacharya, M.J. Schulz, Sens. Actuators B 123 (2007) 177–182.
[22] J. Okunoa, K. Maehashi, K. Kerman, Y. Takamura, K. Matsumoto, E. Tamiya, Biosens. Bioelectron. 22 (2007) 2377–2381.
[23] A.J. Bard, L.R. Faulkner, Electrochemical Methods (Fundamentals and Applications), 2nd edn, John Wiley & Sons, New York, 2000.